Jurnal Tribologi 30 (2021) 116-132

MYTRIBOS Malaysian Tribology Society

Jurnal Tribologi

Website : jurnaltribologi.mytribos.org e-issn: 2289-7232

Cold extrusion using biodegradable oil as lubricant: Experimental and simulation analysis

Aiman Yahaya *, Syahrullail Samion, Nurul Aini Mohd Ahyan, Mohd Kameil Abdul Hamid

School of Mechanical Engineering, Faculty of Engineering, Universiti Teknologi Malaysia, 81310 UTM, Skudai, Johor, MALAYSIA.
*Corresponding author: wmaiman91@gmail.com

KEYWORDS

Palm oil
Tribology
Cold forward extrusion
FEM simulation
Friction

ABSTRACT

Due to various growing concerns on environmental damage caused using non-biodegradable mineral oils, there is a growing awareness globally of the need to promote the use of renewable materials such as vegetable oils. Because of their unique features, such as being non-toxic and biodegradable, vegetable oils have the potential to replace mineral oils as a lubricant. Lubrication is seen as important for controlling the wear and friction of the interacting surfaces as well as in reducing the load applications during the metal forming process, this research had therefore attempted to study the possibility of using palm oil (RBD palm stearin and RBD palm kernel) as a bio-lubricant by benchmarking their performances against those of the additive-free paraffinic mineral oil VG460. This experiment had utilised a cold work plane strain extrusion apparatus with a pair of taper die and a symmetrical work piece (billet) that was constructed from the A1100 annealed pure aluminium with a 5mm radius of deformed area. By comparing the friction behaviours at certain stroke levels and the effects from the billet's effective stresses experiment with the simulated FEM results of high extrusion loads, the palm kernel and palm stearin were found to have not resulted in any severe wear on the product surface hence, indicating their potential to be used as a mineral oil replacement.

Received 6 July 2021; received in revised form 13 August 2021; accepted 25 August 2021.
To cite this article: Yahaya et al., (2021). Cold extrusion using biodegradable oil as lubricant: Experimental and simulation analysis. Jurnal Tribologi 30, pp.116-132.

1.0 INTRODUCTION

The research and development of alternative renewable lubricant that was prompted by the depleting trend of conventional and non-renewable petroleum-based products had led to the discovery of vegetable oils as being one of the most promising alternative and renewable sources as study by Rasep et al., (2021) that use vegetable oils (soybean oil) as a bio-lubricant in U.S, besides that, Golshokouh et al., (2014) also has study the biodegradable material that using the Jatropha oil as a renewable source of lubricant, from both of the result obtain it show that vegetable oil has a possibility to perform well when comparing with the mineral based oil. For this reason, the superior biodegradability level of the vegetable oils had not only given rise to the increased interest of using them as fuel and industrial lubricants, but its natural oil and fat contents had also rendered it to be part of an important food product. According to Lathi & Mattiasson, (2007), reported earlier those unsaturated fatty acids in vegetable oils can be used as metal working fluids and lubricating additives to eliminate corrosion from chlorine containing compounds. Sapawe et al., (2016) also has agree the unique chemical properties of the vegetable oil that absent in mineral oil has a great potential for vegetable oil to lubricate at higher viscosities indexes.

Of all the vegetable oils, the palm oil had been one of the most popularly studied raw material as shown by the investigations conducted on their usage as test lubricants Masjuki and Maleque (1997) investigated the anti-wear properties of palm oil methyl ester (POME), finding that POME functioned as an additive and enhanced anti-wear properties. However, Maleque et al., (2000) state that it only valid at lower loads (up to 500 N) and temperatures (up to 100°C), the wear rates under 5% POME lubricant are lower, whereas at higher loads and temperatures, the wear rates are higher. Farhanah & Syahrullail (2016) investigated the impact of mechanical parameters on the tribological performance of refined, bleached, and deodorised palm stearin. Based on their findings, RBD PS has a superior friction constraint reduction than additive-free paraffinic mineral oil.

Extrusion is one of the most important elements of metal part manufacture. Since excessive friction not only leads to heat generation, wear and the galling of tool surface that will subsequently result in the tools' premature failure, but also the consequence of defective finished products from its increased deformation inhomogeneity, most of the metal forming processes had therefore attempted to mitigate these issues by incorporating the use of lubricants as a way of prolonging the respective tool's life and improving the quality of the finished product (Hafis et al., 2013; Syahrullail et al., 2013). According to Akchurin et al., (2017), the type of lubrication regime used in a metal forming operation has a significant impact on frictional conditions as well as other critical parameters including tooling wear rate and product surface finish.

According to Groche, P. et al. (2018), numerical simulations are essential for an efficient design of modern process chains, where the quality of the gained results is influenced by the input parameters of the numerical model. The friction measurement on the contact interface is directly related to the internal stresses during plastic deformation. The accuracy of the load-displacement experimental findings depends on the performance of the cold extrusion processes in understanding the friction activity at the die-billet wall in which it has to be related primarily to material characteristics (Hafis et al., 2013; Rasep et al., 2021). A friction model is one of the fundamental input boundary conditions in finite element simulations, according to Tan, X. (2002). The friction model is said to be crucial in managing the accuracy of required output outputs projected. For this reason, the Finite Element method that were used by Nagaraj et al. (2019) and Kiu et al., (2018) in their respective studies were found to have accurately predicted the cold

forging die life as well as the simulation of the 3C micro-pin forward extrusion and forging processes.

This research had not only successfully simulated the forward micro-extrusion of a work piece from its input parameters such as material description and frictional behaviour and highlighting the differences between the simulated and the experimental processes but was also able to determine the effective stress-strain and material flow properties after the extrusion as well as the upper punch reaction of the formed material. Therefore, by using the Finite Element Method (FEM), this paper had aimed to assess the metal forming lubricant ability of the different type of palm oil and mineral oils through a comparison of their respective extrusion load, surface roughness and viscosity levels.

2.0 MATERIALS AND METHODS

2.1 Test Material

Figure 1 shows the material tensile test for before and after annealing the pure aluminium, the tensile strength is decreasing from149.27228 MPa to 138.77036MPa, but the modulus of elasticity is remaining the same at 61.785GPa. Table 1 shows the mechanical properties of the billet and taper die. The billet material, which had been milled to 4.5 mm of thickness with a corresponding width and length of 15 mm and 80 mm, is made up of pure aluminium (JIS-A1100) that had been cut from the A1100 pure aluminium (size 30mm x 20mm x 5mm) plate via the CNC-Wire cut EDM machine. Besides adapting well to the cold extrusion process, where the control of extruded aluminium grain structures is driven by the many applications of various industries, aluminium is also known to possess great machinability, excellent thermal and electrical conductivity as well as being resistant to erosion as stated by Misirli, (2010) and Kumar et al., (2021).

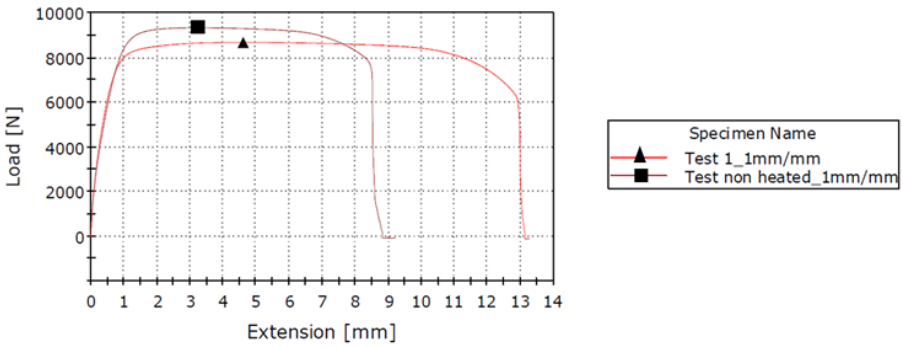

Figure 1: Tensile test for pure aluminium and annealed pure aluminium.

A die with a T45 half angle was chosen to simulate the high frictional condition between the contacting surface of the taper die and billet as a way of preventing the occurrence of a dead metal zone. Since a bigger angle can result in the possibility of even lower frictions, the evaluation on the lubricant's performance would therefore be meaningless if a smaller level of friction is used. Figure 2 shows the schematic geometry of the experiment setup.

Table 1: Die and billet detail

Part	Material	Hardness	Tensile strength (MPa)
Extrusion taper die	SKD11 tool steel	Before heated=40.0 HRC After heated=63.5 HRC	Before heated=308.0 After heated=488.9
Billet	A1100 pure aluminium	44.6 Hv	Not annealed=149.2723 Annealed=138.77036

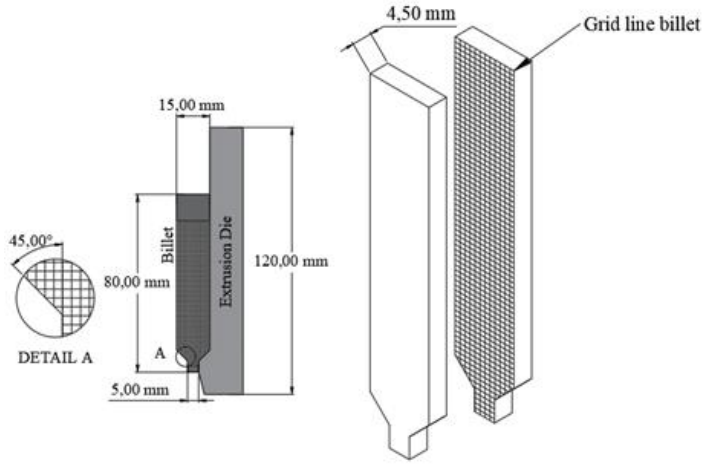

Figure 2: Schematic geometry billet and extrusion die and the stacked billet.

2.2 Sample Lubricant

Palm oil can be divided into two main fractions: one liquid oil (65–70%) olein and one solid fraction (30–35%) stearin (Kellens et al., 2007). Palm oil is rich in C16:0 and C18:1 fatty acid while palm kernel oil has a high concentration of C12:0 fatty acids; this compound is followed by large amounts of other short and medium chain acids (C8:0, C10:0, and C14:0) but small levels of C16:0 and C18 fatty acids (C18:0, C18:1, C18:2) (Gibon, 2012). Palm kernel oil is also heavily saturated relative to palm oil; the saturated fatty acid content of palm kernel oil is typically above 80 percent, while in palm oil it is just ~50 percent. Mono-unsaturated fatty acids count in palm (high IV) and palm kernel oils (Low IV) for ~40% and ~15% and poly-unsaturated for ~10% and ~3% respectively (See Table 2).

Table 2: Fatty Acid Composition (FAC) of Palm stearin, palm kernel oils and palm mid-olein.

FAC (% by gas chromatography)	C8:0	C10:0	C12:0	C14:0	C16:0	C18:0	C16:1	C18:1	C18:2	C18:3	C20:0	C20:1	C22:0	C24:0	SFA	MUFA	PUFA	IV
PS	N.D	N.D	0.16	1.16	54.31	4.71	N.D	32.31	6.68	0.3	0.37	N.D	N.D	N.D	60.71	32.31	6.98	33
PKO	3.6	3.5	47.8	16.3	8.5	2.6	N.D	15.3	2.4	N.D	N.D	N.D	N.D	N.D	82.3	15.3	2.4	17.8

*N.D=Not detected: SFA: saturated fatty acids; MUFA: monounsaturated fatty acids; PUFA:polyunsaturated fatty acids; IV :Iodine Value

The evaluation on the possibility of oil palm being used as a metal forming lubricant substitute in the extrusion process was performed by investigating the lubricity performance of both the RBD palm kernel and RBD palm stearin. In order to observe the potential of the palm oil as extrusion oil 2 types of mineral oil-based lubricant is used as a benchmark, that is commercial extrusion oil (CEO) and high viscosity grade of free paraffinic mineral oil (PMO) VG460. The physicochemical properties of the respective lubricant samples are shown in Table 2. To study the effect of the viscosity on extrusion test VG460 is used as the viscosity grade of the mineral oil-based is very high that act as a benchmark lubricant.

Table 3: Physicochemical properties of sample lubricant.

Properties	Viscosity Grade (mm^2/s)			Density (g/cm^3)
	27°C	40 °C	100 °C	
RBD Palm kernel	46.14	31.32	8.00	860
RBD Palm sterin	48.29	38.01	8.56	870
CEO	107.71	42.05	11.20	900
VG460	1374.60	411.25	28.10	860

2.3 Experiment Set Up

The set-up of the experimental forward extrusion, which had consisted of the workpiece (billet) main components, taper die and container wall as illustrated in Figure. 3 and was performed with a hydraulic press machine at a room temperature level and the respective palm kernel, palm stearin and VG460's. Once the fully assembled plain extrusion apparatus had been placed on the load cell, the readings on the load extrusion (Y-axis) that had occurred along with the puncher movement of each test as well as the ram stroke (X-axis) displacement values from the attached displacement sensor at the plain extrusion apparatus holder were then recorded down before the test was terminated at a piston stroke of 40 mm with an expected steady state condition of the extrusion process as shown in Figure 2.

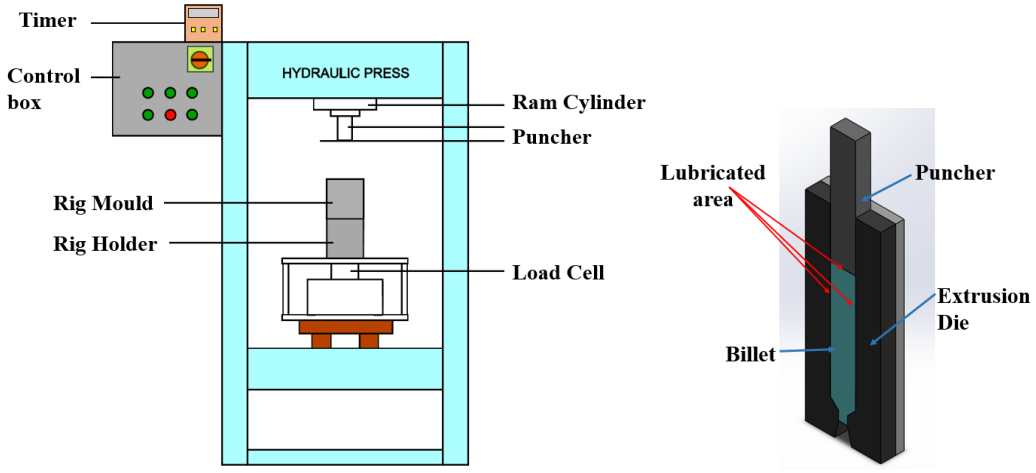

Figure 3: Hydraulic machine and schematic diagram for cold forward extrusion test.

2.4 Finite Element Method

The billet and the actual dimension of the die model that had been created by the CAD software and were exported into the FEM simulator as a way of gauging a more realistic friction condition that had occurred between the surface and the billet. While the billet had been grounded into a fine mesh to ensure a more accurate FE analysis as tabulated in Table 4, the puncher and die on the other hand, were set as a rigid surface without any deformed circumstances during the extrusion process. Figure 4 shows the effects from before and after the cold forward extrusion process.

Table 4: Simulation parameter.

ANNEALED AND WORK-HARDENED	Analysis Options	FEA Program	Scientific Forming Technologies Corporation (SFTC)
		Compiler for User Subroutines	DEFORM-3D Ver-10.2
		Material Plasticity Method	Elastic-Plastic formation
		Die Material Type	Rigid
		Punch Velocity	1mm/s
		Number of steps	350
		Iteration Method	Newton-Raphson
		Remeshing	Global remeshing, overlay quad type, depends on element distortion,
		Number of meshing	32000
		Deformation	Active in FEM + meshing
		Temperature	20°C
	Contact	Inter-Object Data Definition	Shear friction model
		Relative Sliding Velocity	Default (=0)
		Tolerance	0.0255
	Material	Model	
		Young's Modulus	AA1100=61.785 GPa
		Poisson's Ratio	AA6061=0.33

In the current simulation, the coordinates system was perpendicular to the y-axis, and the other two were x-axis and z-axis, respectively. For the extrusion process, the puncher, which was the primary part, is set to a movement speed along the negative y-axis, while the billet is put at the bottom of the puncher as shown in Figure 4. The step is set up to 40mm stroke to merge with experimental stroke, with a single step view to study every move, damage, velocity and also stress effective of the billet. A few seconds passed between the billet touching the lower anvil and the start of forging, and this time-interval had to be taken into account, since it would have an impact on the billet's temperature distribution.

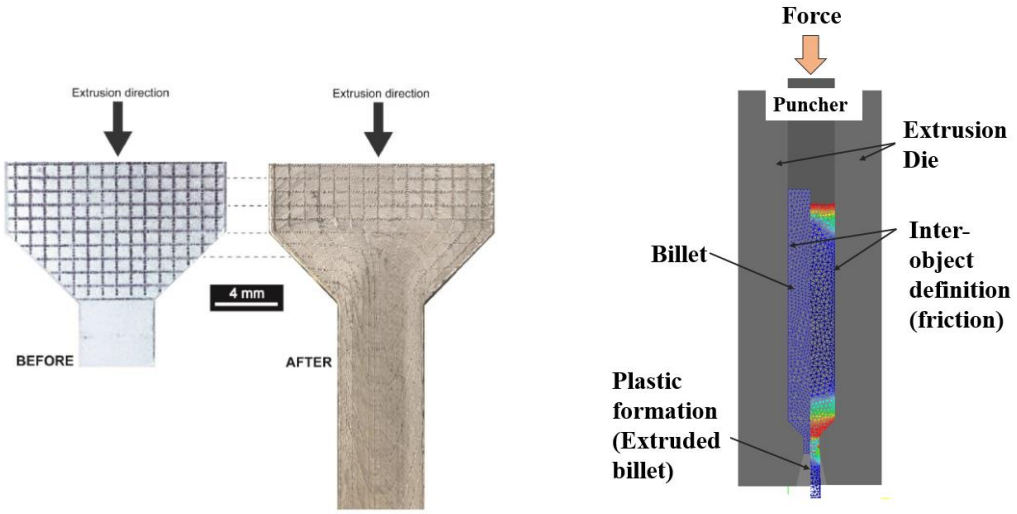

Figure 4: The mechanic of cold forward extrusion process of undeformed and deformed shape.

3.0 RESULTS AND DISCUSSION

3.1 Experimental Result and Friction Coefficient

By observing the effects from the extrusion load experienced by all the sample lubricants in Figure 5, it could be seen that the VG460's piston stroke had reached the steady state condition at 15 mm, where its steady extrusion load towards the 40 mm piston stroke had been between those of 40 kN to 50.51 kN. As for the palm kernel and palm stearin however, they were found to not only reach the steady state conditions after passing the 30 mm piston stroke mark, but the palm kernel and the palm stearin had also experienced a respective higher and lower extrusion load after reaching the 27 mm piston and the 30 mm piston stroke levels.

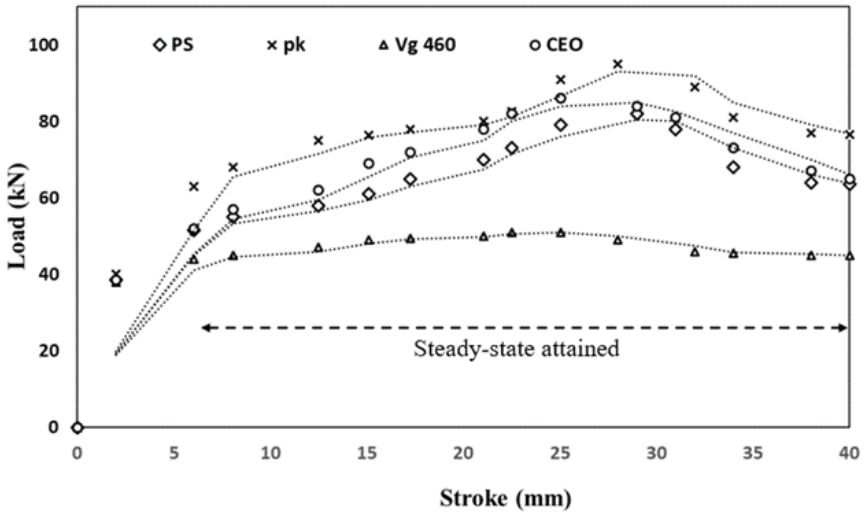

Figure 5: Experimental Graph of load against stroke with friction coefficient.

Based on the simulated friction that was conducted on all the sample lubricants in Figure. 6, VG460 experimental test has the friction behaviour occurring close to m=0.4. The results that were obtained from the palm stearin however, had indicated a massive fluctuation from those of the VG460 with stable loads. As indicated by the results of the FEM simulation test in Figure. 7, the commercial extrusion oil (CEO) and palm stearin was found to have exhibited a friction behaviour m=0.45 at 0-6mm die stroke, and the friction is increase to 0.55 as the die stroke from 6-15mm. However, after 15mm we can see that the CEO has start to increase the friction at m=0.60 until the die stroke 34mm. Palm stearin shows a late fluctuation where the friction is increase at 21mm die stroke until 34mm. In addition, the friction is keep decreasing after the 34mm. From overall observation we can see that the palm stearin has a lower load that generates a slightly lower friction when compared to the CEO. The high force extrusion top die of the palm kernel was also observed from Figure.8, where its initial friction stage that had occurred at m=0.5, was discovered to have increased until m=0.65 at the 26-32mm stroke until an extrusion stability with a friction of 0.6 was reached after the 36mm stroke. It is also important to note that these fluctuations had been mainly due to the squeezing of the lubricant that was generated by the sharp edges of the T45 half angle from the taper die.

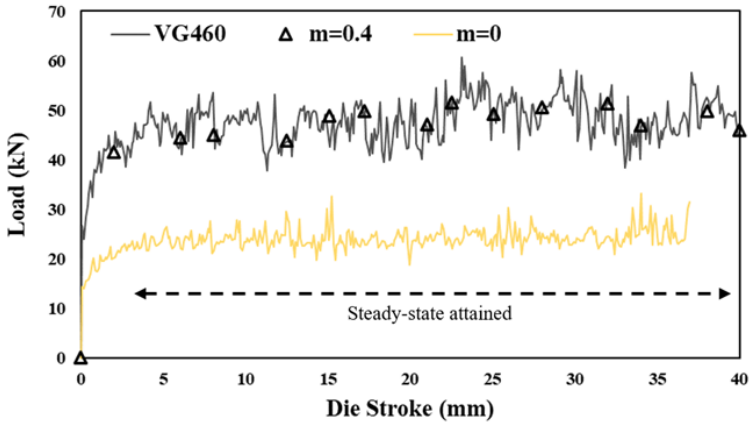

Figure 6: Comparison of simulation for VG460.

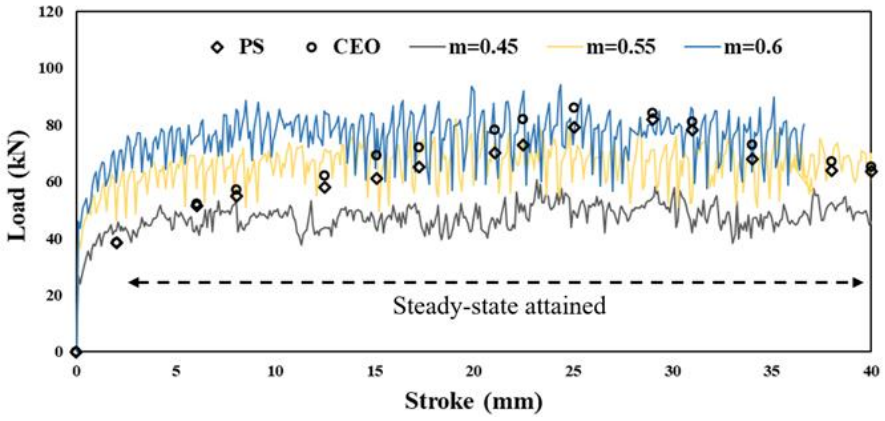

Figure 7: Comparison of simulation for palm sterin and CEO.

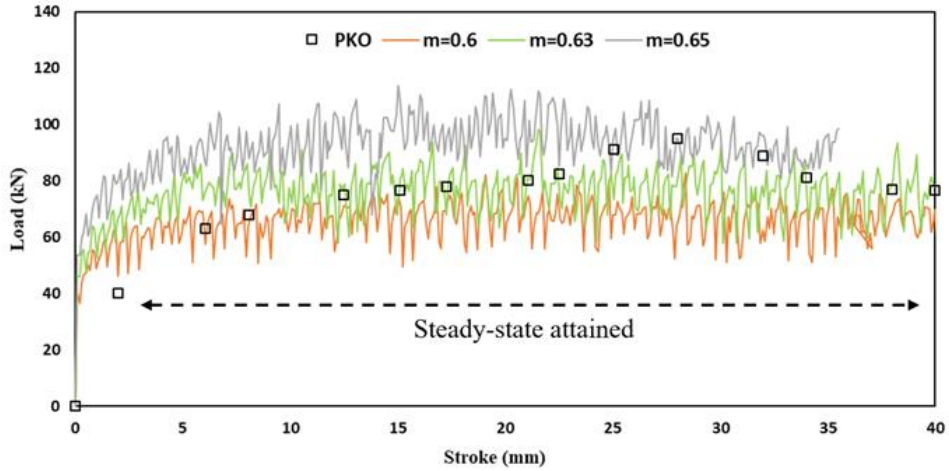

Figure 8: Comparison of simulation for palm kernel

Although the oleic acid and the absorption of free fatty acid (FFA) from the palm oil could help in reducing the sliding friction as discussed by Aiman & Syahrullail, (2017) and Yahaya et al., (2020) as well as maintaining a thin lubrication layer between the taper die and billets, but when compared to the mineral oil, it would still bear the brunt of a higher load effect from the extrusion process. The increasing of force for palm kernel oil indicates that the sample lubricant has poor efficiency in lubricating that will generates a higher friction compared to mineral oil based and palm stearin. This phenomenon may be due to the fatty acid chain inside PMO and PKO is easily broken compared to PS that lead to a higher metal-to-metal contact. According to Afifah et al., (2019), the fatty acid chain has helped the palm oil-based lubricant to reduce the metal-to-metal contact, and will reduce the friction during fourball test. These results had been in line with the findings conducted by Syahrullail et al. (2005; 2011), where they had proven the VG460 as having a better lubrication performance during the metal forming process. According to Azman et al., (2019) and Behrens, (2018), the lower friction level that was experienced by the palm stearin could have been due to its higher kinematic viscosity, while the palm kernel (PK) that had seemed to have more contact with the sliding surface, had implied the requirement of additional energy for shearing the material and ultimately, the increase of its extrusion load. These findings had also been consistent with the results garnered by Hafis et al. (2012; 2013) where they had found the surging of extrusion loads to be related to the friction coefficients of the experimental and finite element (FE) analyses.

3.2 Effects of Taper Die's Patterns and Test Lubricants on Metal Flow Pattern of Extruded Billet's Surfaces

The deformed metal zone that was observed from the changes of the grid line pattern angles, which had been described earlier on the billet plane surface was then compared with the vertical and horizontal flow lines of the tested lubricants by tracing the actual images of the grid lines that had appeared on the T45 extruded billets as shown in Figure 9. From the comparison of the experimental vertical grid lines exhibited by the T45 taper die as shown above, the palm kernel grid lines were found to have situated behind those of the palm stearin and VG460 lubricants,

while the CEO grid lines had seemed to experience more deformations than the VG95, VG460, palm stearin and palm kernel.

The experimental result of metal flow is then shown using the finite element method in terms of total velocity flow (X, Y, and Z-axis) and may be represented as illustrated in Figure 10. From the analysis, we can see that the velocity of the billet for VG460, has a lower total velocity of metal flow. Palm kernel oil however shows the highest velocity of metal flow inside the billet. The increase of friction has increased the load and subsequently increase the velocity of the billet during the compression.

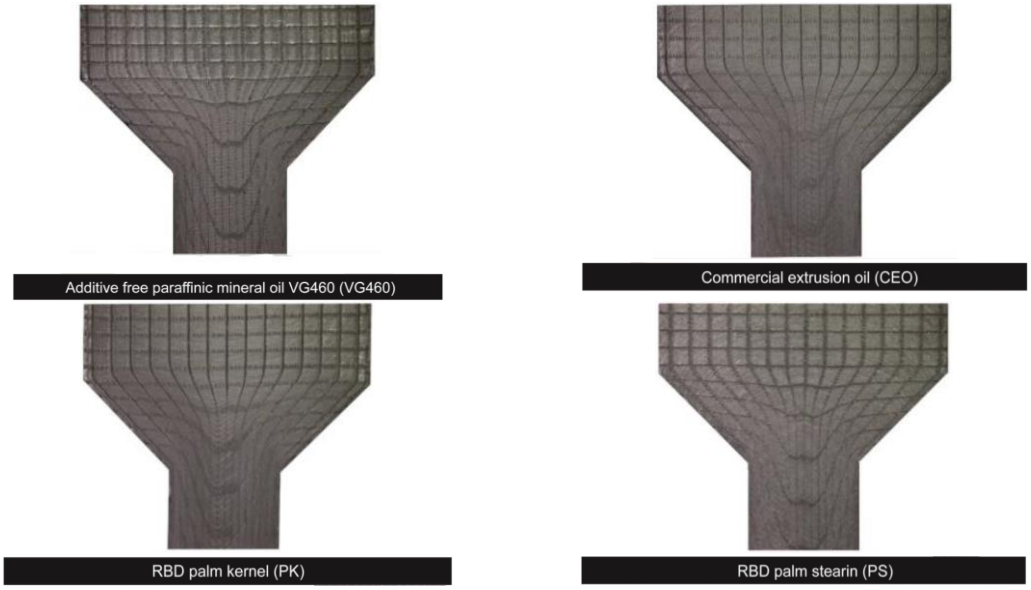

Figure 9: Experimental metal flow comparison of an extruded billetT45.

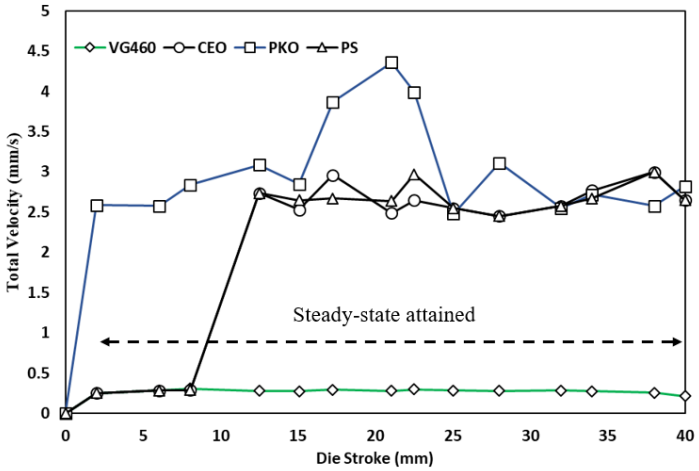

Figure 10: The total maximum velocity inside the billet of all sample.

As reported by Yan et al., (2018) a higher fictional force is known to result in a greater distortion level in extrusion process, the magnitude of the frictional force from the cylinder shape extrusion process was thus found to have led to the formation of a larger deformed metal layer between the outer surface and half of the radius level, this statement is supported by Wang et al., (2012) that summarize from the previous researcher in extrusion process. For this reason, the appearance of these wave-like grid line profiles on the billet were revealed to have been caused by the rapid metal flow of the restricted side billet movement from the frictional force that was created between the billet and the taper die contact.

As shown in Figure 10, although the greater amount of deformed T45 vertical grid lines from the palm kernels had indicated the occurrence of a higher friction between the sliding contact surfaces of the taper die and billet than those of the VG460 and palm stearin, the metal would however, experience a similar deformation level with the other taper dies and test lubricant conditions upon the cessation of the extrusion process.

3.3 Stress Effective

Stress in one of the important analysis studies in order to observe the material behaviour under different sample lubricant (VG460, CEO, PS and PKO) that contribute to a different friction condition. Some of the stress analysis also help the researcher to predict the fracture or cracking to the workpiece as mentioned by (Zhan et al., 2020). Figure 11 shows the result of the stress effective of palm oil based that been compared to the mineral oil based. From the result obtain we can see that VG460 has a very low stress effective on entire stroke compared to other sample. Palm stearin however shows a lower stress effective at 46.8 MPa compared to CEO that has maximum stress of 47.8MPa and PKO with a maximum stress of 58 MPa. The trend of the graph effective shows that the stress is decreasing after 32mm die stroke. At 0-15mm die stroke PKO shows a high stress effective under compression and the stress is due to the high friction inside the tools compare to PS that has a lower friction and generate slightly lower stress.

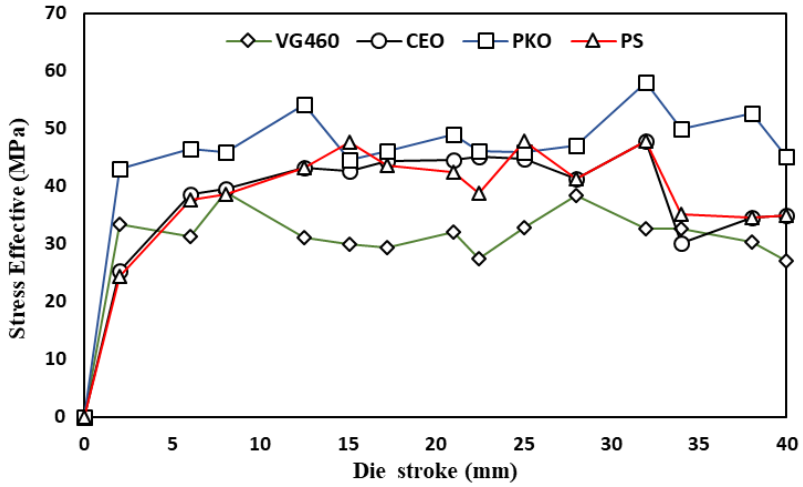

Figure 11: Average stress effective inside the billet.

Die Stroke (mm)	Friction			
	VG460	CEO	PS	PKO
8	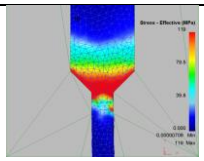	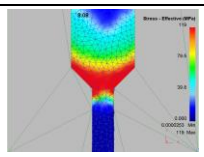	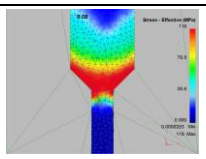	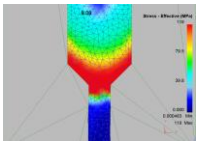
17	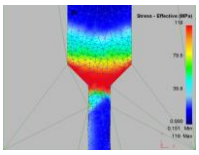	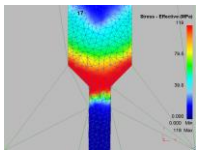	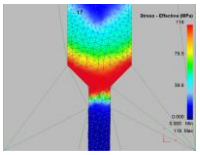	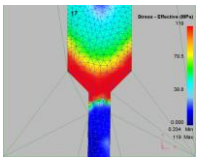
21	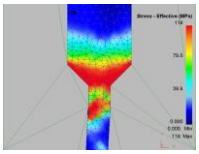	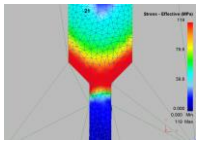	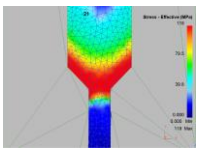	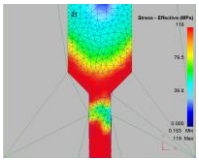
38	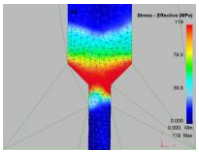	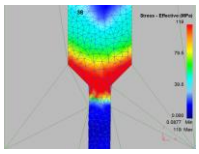	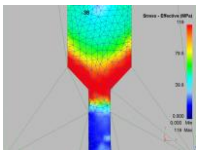	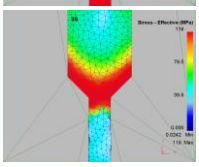

Figure 12: Stress effective at different stroke and friction.

Figure 12 shows the stress effective distribution depicted by the 4 different strokes at different sample lubricant and be taken at different friction condition. From the result obtain it was observed that a more inconsistent stress distribution had existed at the output die of the cold forward extrusion process during the deformation stage with the highest FEM stress value reading of 119 MPa highlighted in the red region. The stress distribution is shows that as the die stroke is higher, the stress distribution is getting bigger and effect high area to all to the billet part. When observing into the lubricant sample, VG460 has a less stress distrbution compared to the palm oil based lubricant. PKO has shown the highes effect of the surface stress on the billet where at the 38mm die stroke the stress distribution became larger due to the higher friction as the PKO is less effective in lubricating under the extrusion process compre to the PS.

According to Tiong et al., (2012), at room temperature, RBD palm stearin is semi-solid, but once it hits 40°C, it will fully liquidise. and it may exhibit slow motion during the extrusion process. This physical state results in less friction during the process and less compression load. Less metal-to-metal interaction between the work piece and the die was then reported. Dong et al., (2018), also shared the importance of lubricity for reducing the stress effective distribution at the billet where he had described the difference of the metal flow patterns during the extrusion process as being attributed to its dominant friction during the extrusion process. According to Maeno et al., (2017) the new material flow characteristic that was yielded from the backward extrusion process was also discovered to be affected by the unexpected constellation of individual grains and the consequent inhomogeneous local deformation, as a result, the distribution of process parameters and its pressure characteristic increases.

3.4 Surface Roughness and Observation on Experimental Surfaces of Extruded Billet

Since the product area of the end product quality is regarded as an important aspect for actual industries, a comparison on the roughness value of the extruded billet's product area was thus conducted as shown in Figure. 13, where the product area, which is the billet's region that had been extruded from the taper die bearing, was measured from the direction that had been perpendicular to the extrusion direction.

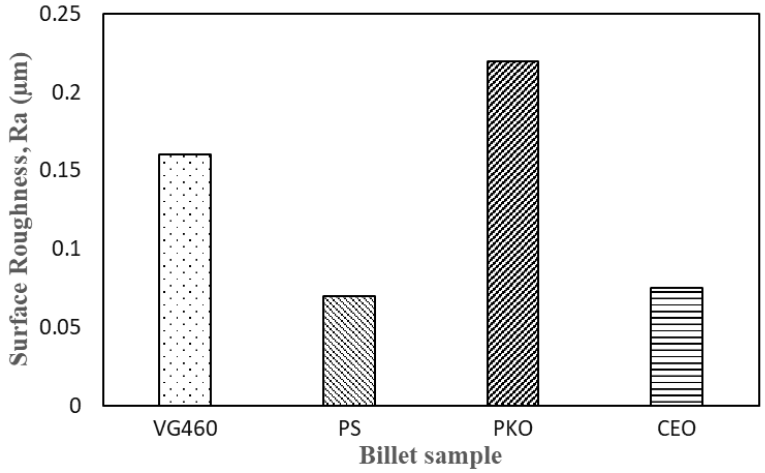

Figure 13: Surface roughness of an extruded billet on the product area.

The product, deformed area, and un-deformed areas were classified into three sections in the contiguous or observation area between the billets and taper dies. The results from this comparison study had not only shown the palm stearin as demonstrating a better surface roughness performance than those of the VG460 oil sample, because of the fatty acid that had helped maintained the layer between the taper die and billets as proposed by Quinchia et al., (2010), but also its higher viscosity level that was reflected from the finer surface roughness of the T45 taper die than those of the palm kernel's. For this reason, since the RBD palm kernel (PK) and the commercial extrusion oil (VG460) are considered as lower viscosity lubricants, they are seen as having a high inclination for supplying lubricants from an un-deformed area to the product area, while those of the palm stearin had remained on the sliding contact area surface because of their highly physical characteristic with a high concentration. As a result, the reduced roughness value at the sample part could have been caused by the section's higher contact pressureHigh values of the frictional coefficient, according to Alamer et al., (2018), resulted in larger form deviations in the extruded component due to higher compression load at the die work piece.

The image of the experimental extruded billet from the T45 taper die as depicted in Figure 14 had indicated the high metal-to-metal contact surfaces of most viscous lubricants as leading to the higher friction and wear levels. As such, it can be surmised that the increment of real contact area would enhance the creation of smoother surfaces, while the rougher surfaces are caused by the smaller contact area of the interlocked asperities.

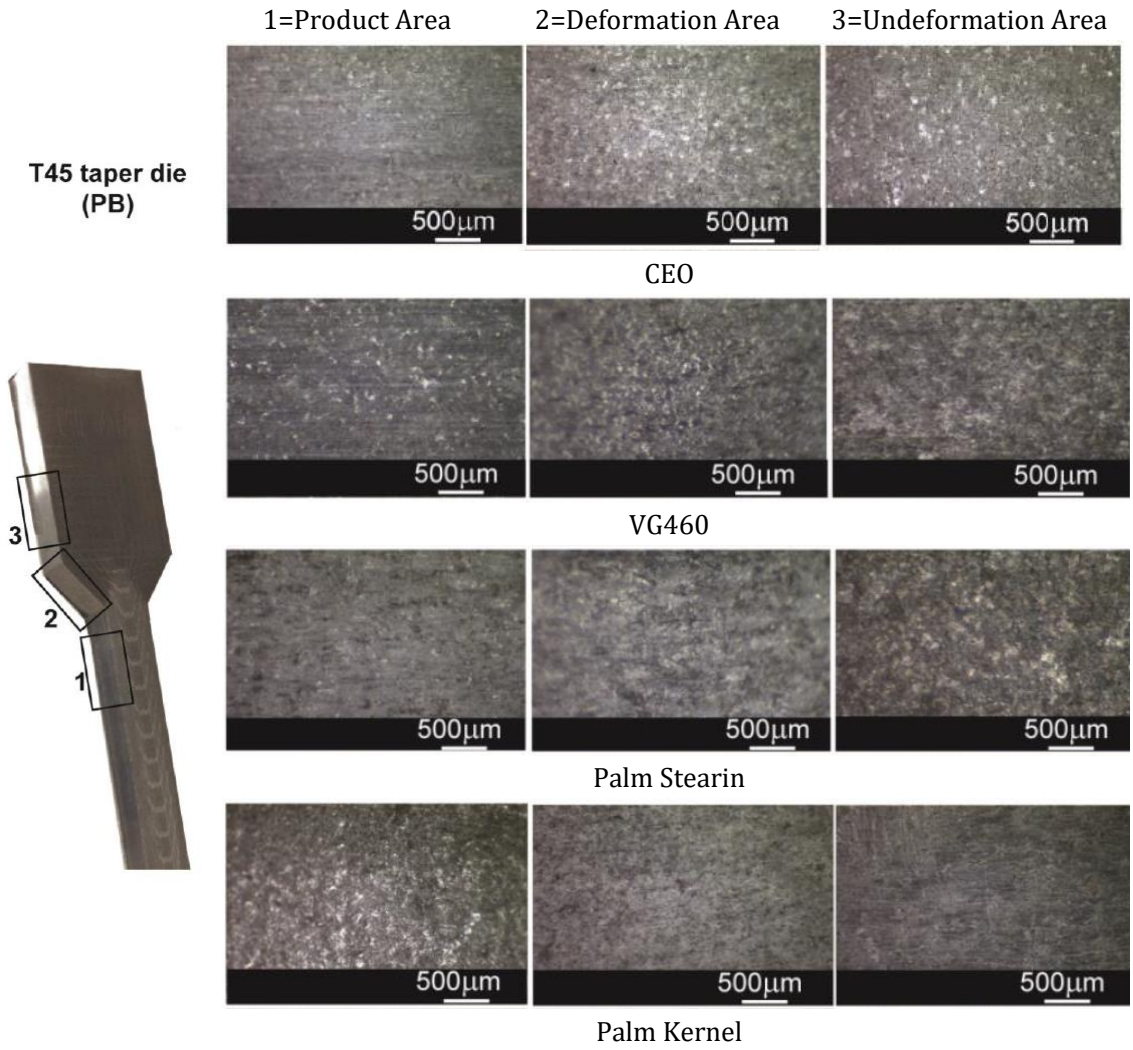

Figure 14: Experimental surfaces of an extruded billets for T45 taper die.

4.0 CONCLUSION

Finite element method (FEM) is used to present an analysis of the friction, metal flow and effective stress on the workpiece. From the analysis it shows that the deformation of the simulation data has been validated to the experiment so that the value of the friction for each sample can be recorded. The palm stearin shows lowest friction value and have improve the lubrication performance by reducing the friction up to 23.1% when compared to the other sample, and it shows that PS has a lower force that may generate a lower friction compared to other palm oil based. The results that were obtained from the entire sample tests also shows that the palm kernel was not only found to have exhibited the highest top die extrusion test force than those of the palm stearin and VG460, but the FEM simulation test had also shown a higher friction behaviour that was caused by the high metal-to-metal contact between those of the billets and

taper die. Palm kernel oil also has the highest stress effective distribution compared to the other sample. In the other hand, the palm stearin also is discovered to have the most desired roughness value as compared to the VG460 and palm kernel samples.

ACKNOWLEDGEMENT

The authors would like to express their thanks to the Ministry of Higher Education of Malaysia for the FRGS Grant (FRGS/1/2018/TK03/UTM/02/14), Universiti Teknologi Malaysia (UTM) for the Research University Grant (21H50) and TDR Grant (05G23).

REFERENCES

Afifah, A. N., Syahrullail, S., Azlee, N. I. W., Sidik, N. A. C., Yahya, W. J., & Abd Rahim, E. (2019). Biolubricant production from palm stearin through enzymatic transesterification method. Biochemical Engineering Journal, 148, 178-184.

Aiman, Y., & Syahrullail, S. (2017). Development of palm oil blended with semi synthetic oil as a lubricant using four-ball tribotester. Jurnal Tribologi, 13, 1-20.

Akchurin, A., Bosman, R., & Lugt, P. M. (2017). Generation of wear particles and running-in in mixed lubricated sliding contacts. Tribology international, 110, 201-208.

Alamer, B., Karataş, Ç., Mert, F., & Aljawad, H. (2018). Effect of lubrication and friction coefficient on temperature distribution for combined backward forward extrusion process for alloy steel. Academic Perspective Procedia, 1(1), 352-357.

Azman, N. F., & Samion, S. (2019). Dispersion stability and lubrication mechanism of nanolubricants: a review. International journal of precision engineering and manufacturing-green technology, 6(2), 393-414.

Behrens, B. A. (2018). Ecological lubrication in cold forming of sintered powder metallurgical components. Dry Metal Forming Open Access Journal, 4, 68-73.

Chew, T. L., Chew, T. L., Bhatia, S., & Bhatia, S. (2008). Catalytic processes towards the production of biofuels in a palm oil and oil palm biomass-based biorefinery. Bioresource Technology, 99(17), 7911–7922.

Chong, Y. Y., Thangalazhy-Gopakumar, S., Gan, S., Ng, H. K., Lee, L. Y., & Adhikari, S. (2017). Kinetics and mechanisms for copyrolysis of palm empty fruit bunch fiber (EFBF) with palm oil mill effluent (POME) sludge. Energy & Fuels, 31(8), 8217-8227.

Dong, Y., Zheng, K., Fernandez, J., Fuentes, G., Li, X., & Dong, H. (2018). Tribology and hot forming performance of self-lubricious NC/NiBN and NC/WC: C hybrid composite coatings for hot forming die. Journal of Materials Processing Technology, 252, 183-190.

Ebrahimi, R., & Najafizadeh, A. (2004). A new method for evaluation of friction in bulk metal forming. Journal of Materials Processing Technology, 152(2), 136-143.

Farhanah, A. N., & Syahrullail, S. (2016). Evaluation of lubrication performance of RBD palm stearin and its formulation under different applied loads. Jurnal Tribologi, 10, 1-15.

Golshokouh, I., Syahrullail, S., Ani, F. N., & Masjuki, H. H. (2014). Investigation of Palm Fatty Acid Distillate Oil as an Alternative to Petrochemical Based Lubricant. Journal of Oil Palm Research, 26(1), 25-36.

Groche, P., Fritsche, D., Tekkaya, E. A., Allwood, J. M., Hirt, G., & Neugebauer, R. (2007). Incremental bulk metal forming. CIRP annals, 56(2), 635-656.

Hafis, S. M., Ridzuan, M. J. M., Farahana, R. N., Ayob, A., & Syahrullail, S. (2013). Paraffinic mineral oil lubrication for cold forward extrusion: Effect of lubricant quantity and friction. Tribology International, 60, 111-115.

Hafis, S. M., Ridzuan, M. J. M., Imaduddin Helmi, W. N., & Syahrullail, S. (2012). Effect of extrusion ratio on paraffinic mineral oil lubricant in cold forward extrusion. AIP Conference Proceedings, 1440(1), 556–561.

Hafis, S.M., Ridzuan, M.J.M., Farahana, R.N., Ayob, A. and Syahrullail, S. (2013). Paraffinic mineral oil lubrication for cold forward extrusion: Effect of lubricant quantity and friction. Tribology International, 60, 111–115.

Kellens, M., Gibon, V., Hendrix, M., & De Greyt, W. (2007). Palm oil fractionation. European Journal of Lipid Science and Technology, 109(4), 336-349.

Kiu, S. S. K., Yusup, S., Soon, C. V., Arpin, T., Samion, S., & Kamil, R. N. M. (2017). Tribological investigation of graphene as lubricant additive in vegetable oil. Journal of Physical Science, 28, 257.

Kumar, P., Nivetha, S. K., Began Peruvazhuthi, S., Raman, K., & VS, S. K. (2021). Characterization and analysis of AA1100-SiCp metal matrix composite fabricated through friction stir processing. Jurnal Tribologi, 29, 31-40.

Lathi, P. S., & Mattiasson, B. (2007). Green approach for the preparation of biodegradable lubricant base stock from epoxidized vegetable oil. Applied Catalysis B: Environmental, 69(3-4), 207-212.

Maeno, T., Mori, K., Ichikawa, Y., & Sugawara, M. (2017). Use of liquid lubricant for backward extrusion of cup with internal splines using pulsating motion. Journal of Materials Processing Technology, 244, 273-281.

Maleque, M. A., Masjuki, H. H., & Sapuan, S. M. (2003). Vegetable-based biodegradable lubricating oil additives. Industrial Lubrication and Tribology, 55(3):, 137–143.

Maleque, M., Haseeb, S. M., & Masjuki, H., (2000). Effect of mechanical factors on tribological properties of palm oil methyl ester blended lubricant. Wear, 239(1), 117–125.

Masjuki, H. H., & Maleque, M. A. (1997). Investigation of the anti-wear characteristics of palm oil methyl ester using a four-ball tribometer test. Wear, 206(1-2), 179-186.

Misirli, C., & Çan, Y. (2010). An experimental study and designing process by using CAD/CAE: in combined open die forging-extrusion process of different shaped geometries from aluminium alloy samples. International Journal of Modern Manufacturing Technologies Review, 1(1), 55-61.

Nagaraj, M., Kumar, A., Ezilarasan, C., & Betala, R. (2019). Finite Element Modeling in Drilling of Nimonic C-263 Alloy Using Deform-3D. Computer Modeling in Engineering & Sciences, 118(3), 679-692.

Quinchia, L. A., M.A Delgado, Valencia, C., Franco, J. M., & Gallegos., C. (2010). Viscosity Modification of Different Vegetable Oils with EVA Copolymer for Lubricant Applications. Industrial Crops and Products, 32, 607–612.

Rasep, Z., Yazid, M. N. A. W. M., & Samion, S. (2021). A study of cavitation effect in a journal bearing using CFD: A case study of engine oil, palm oil and water. Jurnal Tribologi, 28, 48-62

Sapawe, N., Samion, S., Zulhanafi, P., Nor Azwadi, C. S., & Hanafi, M. F. (2016). Effect of addition of tertiary-butyl hydroquinone into palm oil to reduce wear and friction using four-ball tribotester. Tribology Transactions, 59(5), 883-888.

Syahrullail, S., Azwadi, C. S. N., & Ing, T. C. (2011). The Metal Flow Evaluation of Billet Extruded with RBD Palm Stearin. International Review of Mechanical Engineering (I.R.E.M.E), 21–27.

Syahrullail, S., Hariz, M. A. M., Hamid, M. A., & Bakar, A. A. (2013). Friction characteristic of mineral oil containing palm fatty acid distillate using four ball tribo-tester. Procedia Engineering, 68, 166-171.

Syahrullail, S., Nakanishi, K., & Kamitani, S. (2005). Investigation of the effects of frictional constraint with application of palm olein oil lubricant and paraffin mineral oil lubricant on plastic deformation by plane strain extrusion. Japanese journal of tribology, 50(6), 727-738.

Syahrullail, S., Wira, J. Y., Wan Nik, W. B., & Fawwaz, W. N. (2013). Friction characteristics of RBD palm olein using four-ball tribotester. Applied Mechanics and materials 315, 936-940.

Tan, X. (2002). Comparisons of friction models in bulk metal forming. Tribology International, 35(6), 385-393.

Tiong, C. I., Azli, Y., Kadir, M. R. A., & Syahrullail, S. (2012). Tribological evaluation of refined, bleached and deodorized palm stearin using four-ball tribotester with different normal loads. Journal of Zhejiang University Science A, 13(8), 633-640.

Wang, L., Zhou, J., Duszczyk, J., & Katgerman, L. (2012). Friction in aluminium extrusion - Part 1: A review of friction testing techniques for aluminium extrusion. Tribology International, 56, 89–98.

Yahaya, A., Samion, S., Musa, M. N., (2020). Determination of friction coefficient in the lubricated ring upsetting with palm kernel oil for cold forging of aluminum alloys. Jurnal Tribologi, 25, 16-28.

Yan, X., Chen, Z., Qi, A., Wang, X., & Shi, S. (2018). Experimental and theoretical study of a lead extrusion and friction composite damper. Engineering Structures, 177, 306-317.

Zhan, J. M., Yao, X. H., & Han, F. (2020). An approach of peridynamic modeling associated with molecular dynamics for fracture simulation of particle reinforced metal matrix composites. Composite Structures, 250, 112613.